

## Electronic Supplementary Information

# Anisotropic Expansion and Size-Dependent Fracture of Silicon Nanotubes during Lithiation

*Chao Wang,<sup>a,b</sup> Jici Wen,<sup>c,d</sup> Fei Luo,<sup>a</sup> Baogang Quan,<sup>a</sup> Hong Li,<sup>a,b</sup> Yujie Wei,<sup>\*c,d</sup> Changzhi Gu<sup>\*a,b</sup> and Junjie Li<sup>\*a,b, e</sup>*

<sup>a</sup>Beijing National Laboratory for Condensed Matter Physics, Institute of Physics, Chinese Academy of Sciences, Beijing 100190, P. R. China

<sup>b</sup>School of Physical Sciences, University of Chinese Academy of Sciences, Beijing 100049, P. R. China

<sup>c</sup>State Key Laboratory of Nonlinear Mechanics, Institute of Mechanics, Chinese Academy of Sciences, Beijing 100190, P. R. China

<sup>d</sup>School of Engineering Sciences, University of Chinese Academy of Sciences, Beijing 100049, P. R. China

<sup>e</sup>Songshan Lake Materials Laboratory, Dongguan, Guangdong, 523808, P. R. China

### Corresponding Authors

*\*(J. L.) jjli@iphy.ac.cn, (C. G.) czgu@iphy.ac.cn, (Y. W.) yujie\_wei@lnm.imech.ac.cn*

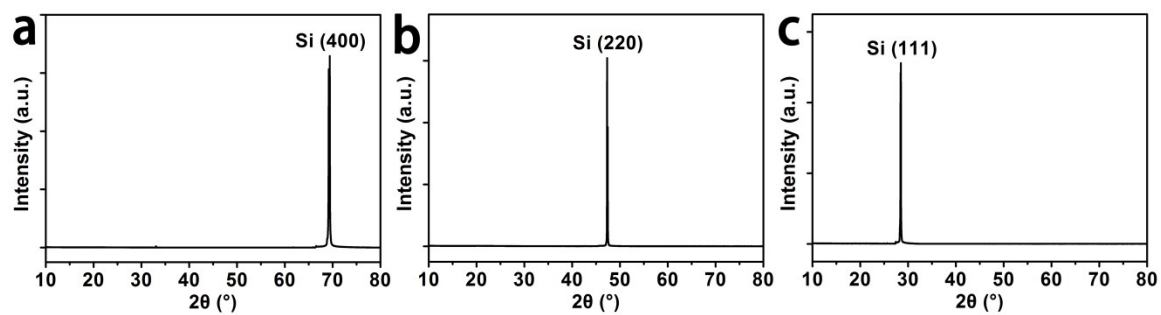


**Fig. S1** XRD spectra of silicon substrates with (a)  $\langle 100 \rangle$ , (b)  $\langle 110 \rangle$ , and (c)  $\langle 111 \rangle$  crystal orientations. The spectra show the typical (400), (220), and (111) diffraction peaks of crystalline silicon, respectively.

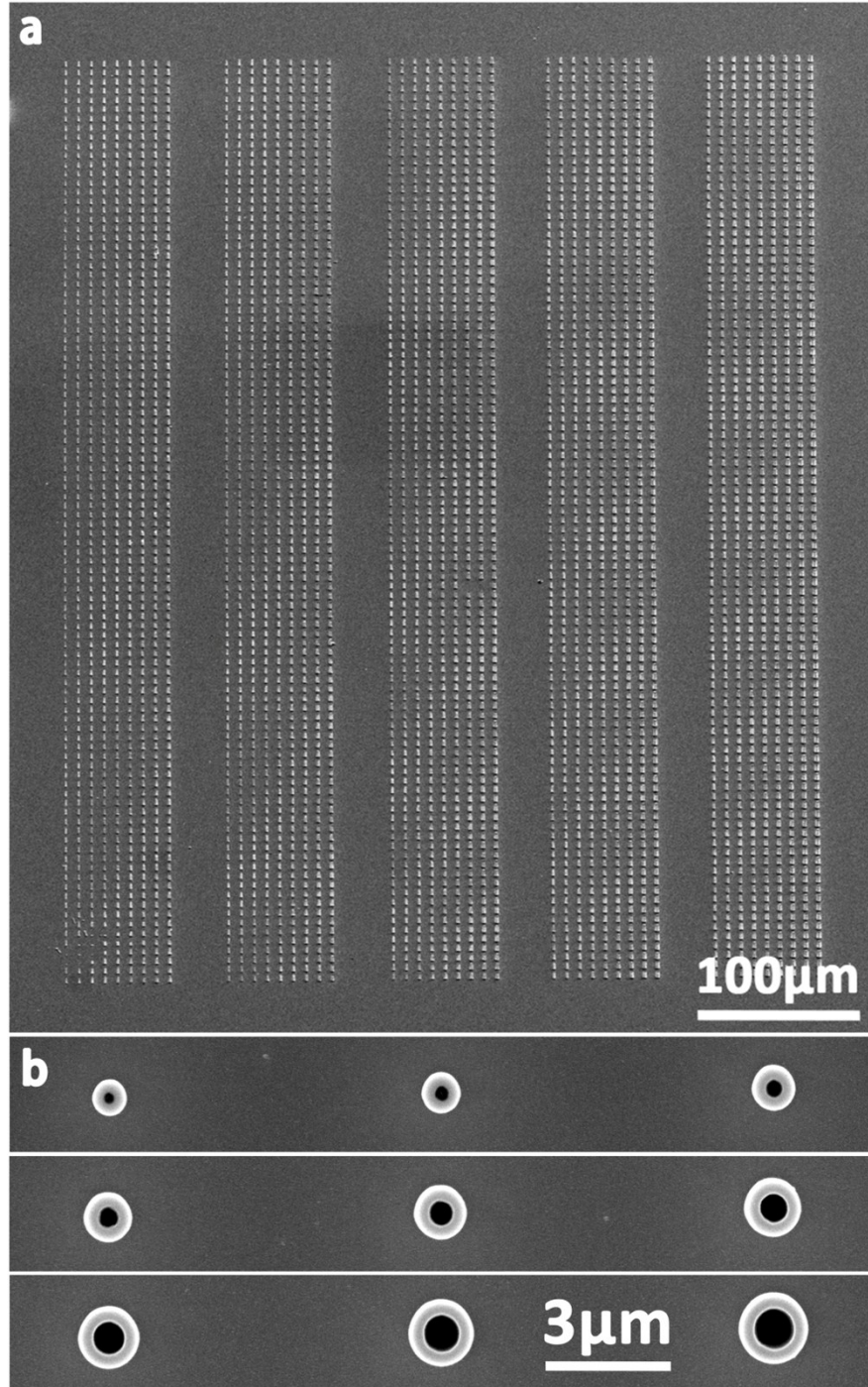


**Fig. S2** (a) SEM image of the whole silicon nanotube arrays showing five arrays with 100 rows. The wall thicknesses of the five arrays are 100, 200, 300, 400, and 500 nm, respectively. (b) SEM images of the silicon nanotubes in a row of the third array (wall thickness of 300 nm) with various inner radii (100, 150, 200, 250, 300, 350, 400, 450, and 500 nm, respectively).

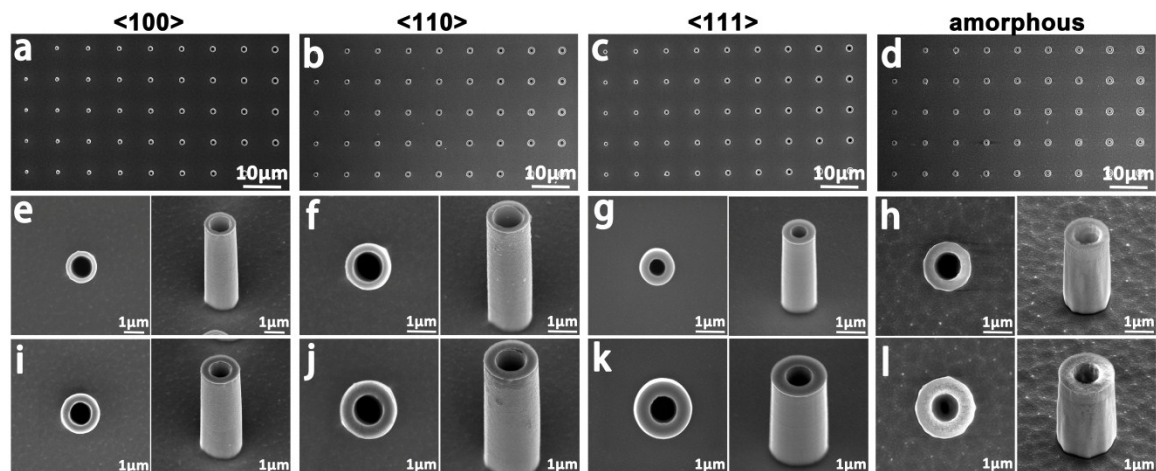


**Fig. S3** SEM images of the pristine  $\langle 100 \rangle$ ,  $\langle 110 \rangle$ ,  $\langle 111 \rangle$ , and amorphous silicon nanotubes before lithiation (corresponding to Fig. 2). (a–d) The silicon nanotube arrays with wall thicknesses of 300, 500, 400, and 500 nm, respectively. (e–h) The smaller silicon nanotubes with wall thickness of 300 nm and inner radii of 500, 500, 300, and 500 nm, respectively. (i–l) The larger silicon nanotubes with wall thickness of 500 nm and inner radius of 500 nm.

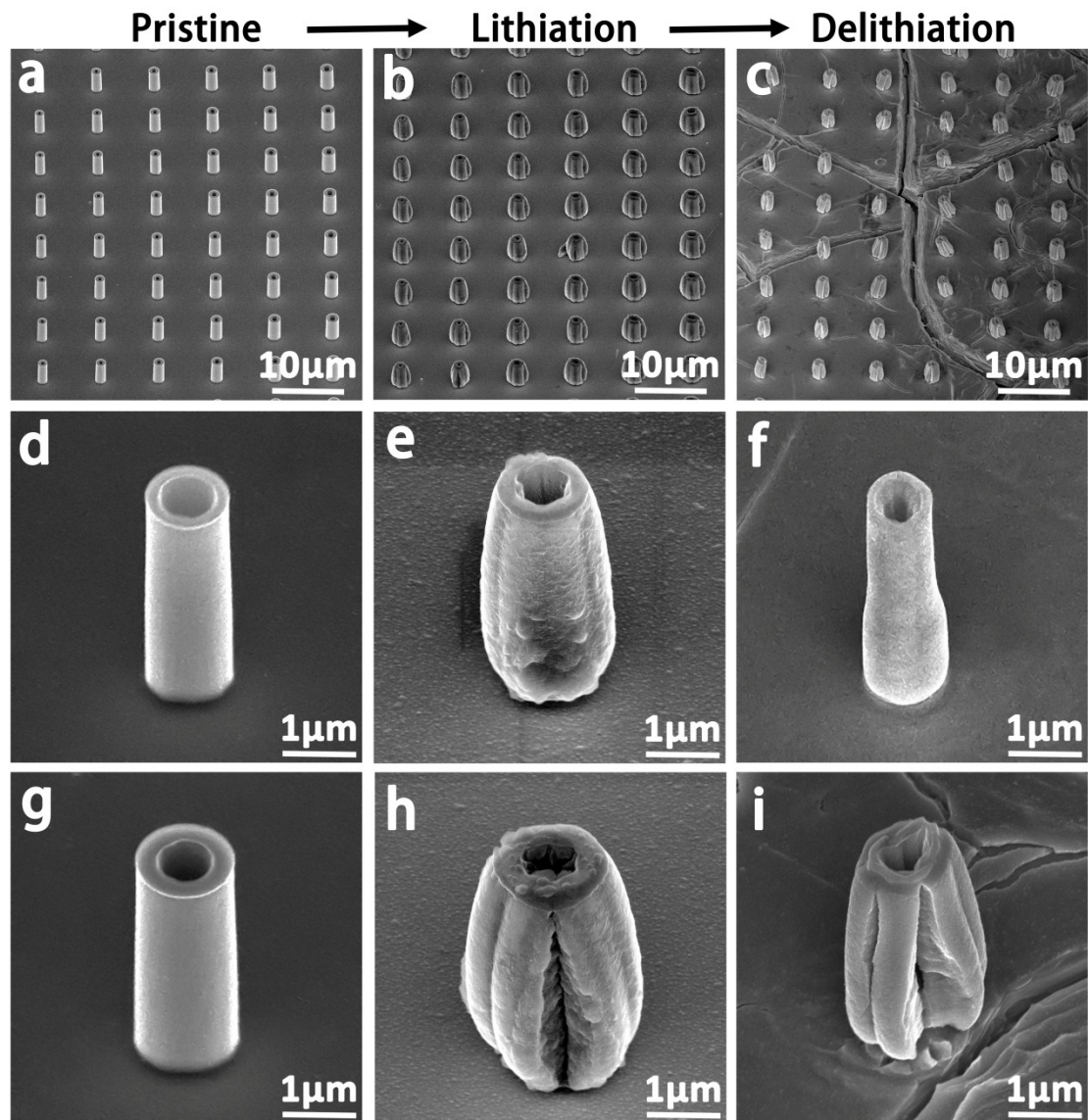


**Fig. S4** Expansion and contraction behavior of  $\langle 111 \rangle$  silicon nanotubes after initial lithiation and delithiation. SEM images of (a–c) silicon nanotube arrays with thickness of 400 nm, (d–f) unfractured silicon nanotubes with thickness of 200 nm and inner radius of 400 nm, and (g–i) fractured silicon nanotubes with thickness of 300 nm and inner radius of 400 nm before electrochemical test (left column), after initial lithiation (middle column), and after initial delithiation (right column), respectively.

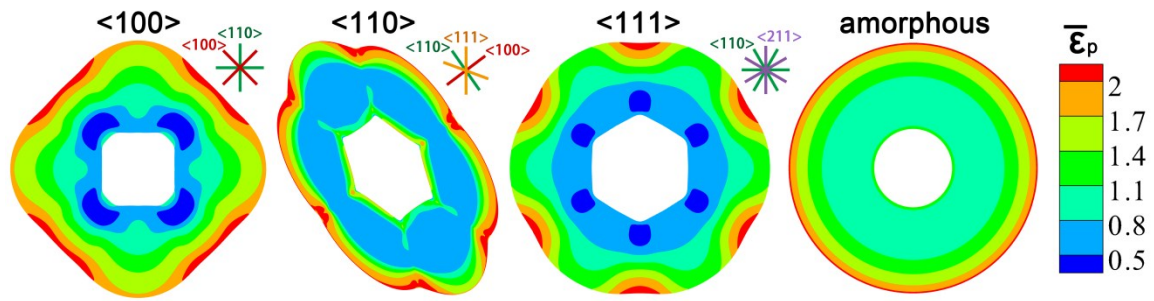


**Fig. S5** Cumulated plastic strain contours of the cross-sections of  $\langle 100 \rangle$ ,  $\langle 110 \rangle$ ,  $\langle 111 \rangle$ , and amorphous silicon nanotubes at normalized lithiation time  $t = 1/3$ .